Modification of the classical nucleation theory based on molecular simulation data for surface tension, critical nucleus size, and nucleation rate

Martin Horsch, Jadran Vrabec,* and Hans Hasse

Institute of Thermodynamics and Thermal Process Engineering,

Universität Stuttgart, Pfaffenwaldring 9, 70569 Stuttgart, Germany

(Dated: July 11, 2008)

Abstract

Nucleation in supersaturated vapor is investigated with two series of molecular-dynamics simulations in the canonical ensemble. The applied methods are: (a) analysis of critical nuclei at moderate supersaturations by simulating equilibria of single droplets with surrounding vapors in small systems; (b) simulation of homogeneous nucleation during condensation with large systems containing 10^5 – 10^6 particles for calculating the nucleation rate of vapors at high supersaturations. For the Lennard-Jones fluid, truncated and shifted at 2.5 times the size parameter, it is shown that the classical nucleation theory underestimates both the nucleation rate and the size of the critical nucleus. A surface property corrected modification of this theory is proposed to consistently cover data on the surface tension of the curved interface, the critical nucleus size, and the nucleation rate.

PACS numbers: 64.60.qe, 68.03.Cd, 82.60.Nh

INTRODUCTION

Homogeneous nucleation during condensation of supersaturated vapors is a well-studied topic; however, it is not yet fully understood despite its general importance. The most widespread modeling approach is still the classical nucleation theory (CNT) [1–4]. CNT is an acceptable approximation for some simple fluids but may yield huge deviations compared to experimental data in other cases [5]. An important source of error is the assumption that the emerging liquid has the same thermodynamic properties as the bulk liquid phase [6]. Condensation processes of practical interest, e.g. in atmospheric science, are usually heterogeneous or ion-induced and have a more complex mechanism of nucleation [7]. However, to adequately describe such processes a thorough understanding of the homogeneous case is a prerequisite.

Experimental methods for studying homogeneous nucleation face considerable challenges: experimentally, a homogeneous system without walls or other irregularities can at best be approximated, a difficulty that is absent in molecular simulation. Furthermore, the experimentally accessible range of the nucleation rate J is limited to comparatively slow processes that are relatively far from the spinodal [8]. Experimental data on the critical nucleus size have only recently become available [9]. In molecular simulation, homogeneous nucleation can straightforwardly be studied by a direct approach where a supersaturated vapor is observed for some time interval, the emerging nuclei are counted, and their size is evaluated [10, 11]. Due to the limitations in computational power, accessible system size and time interval are limited. Thus the direct approach can currently only be applied to vapors at high supersaturations, where nucleation occurs within nanoseconds.

For systems at lower supersaturation it is necessary to follow other, more indirect approaches, e.g. by simulating other ensembles or related systems instead of nucleation in the supersaturated phase itself, which occurs too slowly. Key quantities determined from such indirect simulations are the size of the critical nucleus $n^\star$ and its Gibbs energy of formation $\Delta G^\star$, and methods based on transition path sampling also permit a study of kinetic aspects [12]. Both molecular-dynamics (MD) simulation with inserted nuclei in nonequilibrium with the surrounding supersaturated phase [13] or based on transition path sampling [14] and Monte Carlo (MC) simulation [6, 15] were used for such purposes in the past.

In the present work, both the direct and an indirect simulation approach were applied to

validate two versions of CNT and to develop a new surface property corrected (SPC) modification of CNT. A simple model fluid was chosen, where the intermolecular interactions are described by the Lennard-Jones (LJ) potential, truncated and shifted at an intermolecular distance $r = 2.5\sigma$ [16]. The small cutoff radius leads to relatively fast simulations and avoids long-range corrections that are hard to estimate for inhomogeneous systems [17]. The truncated and shifted LJ potential (LJTS) defines an important and well studied model fluid that can be used to describe noble gases and methane very accurately. A considerable amount of thermodynamic data is available for it and in particular, the dependence of the surface tension on curvature has been quantified [18].

CLASSICAL NUCLEATION THEORY

To describe homogeneous nucleation during condensation, a supersaturated vapor in a volume V at the temperature T and a pressure p which is larger than the saturated vapor pressure p_s is considered. The quotient $\mathcal{S} = p/p_\mathrm{s}$ is called the supersaturation of the vapor (with respect to pressure). Starting from a homogeneous vapor with $\mathcal{S} > 1$, nanoscopic droplets begin to form after some induction time as dispersed nuclei of the emerging liquid phase. They assume a specific size distribution, and the critical nucleus size $n^\star$ is the number of particles n where the Gibbs energy of nucleus formation ΔG_n has its maximal value $\Delta G^\star$ [2].

The size of the critical nucleus and its energy of formation were discussed by Gibbs [1] from a theoretical standpoint. Given that the number of nuclei with n particles is usually determined in CNT by applying a factor of $\exp(-\Delta G_n/k_B T)$ to the number of monomers, an internally consistent approach [19] leads to the expression

$$\Delta G_n = -(n-1)(\mu - \mu_\mathrm{s}) + \zeta_n - \zeta_1. \tag{1}$$

Here, ζ_n is the surface free energy of a nucleus with n particles; μ_s and μ are the chemical potentials of the saturated and the supersaturated vapor. In expression (1) a negative volume contribution competes with a positive surface contribution. The difference between the chemical potentials can be determined from an integral over the pressure along the isotherm of the metastable vapor

$$\mu = \mu_\mathrm{s} + \int_{p_\mathrm{s}}^{p} \frac{dp}{\rho}. \tag{2}$$

Volmer and Weber [2] approximated the nucleation rate by

$$J = C \exp(-\Delta G^\star / k_B T). \tag{3}$$

The preexponential coefficient is [4]

$$C = \frac{A^\star p N_1 \mathcal{Z} \mathcal{N}}{V\sqrt{2\pi m k_B T}}, \tag{4}$$

where $A^\star$ represents the surface area of a critical nucleus, N_1 the number of monomers constituting the vapor,

$$\mathcal{Z} = \sqrt{\frac{-1}{2\pi k_B T} \frac{\partial^2 G_n}{\partial n^2}\Big|_{n=n^\star}}, \tag{5}$$

is the Zel'dovich factor, and m is the mass of a particle. Furthermore, $\mathcal{N} = b^2/(b^2+q^2)$ is the thermal nonaccommodation factor which is calculated from 'the energy released on addition of a monomer' to a critical nucleus 'above that needed to maintain the existing temperature' [4]

$$q = \Delta h_\mathrm{v} - \frac{1}{2}k_B T - \left.\frac{\partial \zeta_n}{\partial n}\right|_{n=n^\star}, \tag{6}$$

and the kinetic energy variance

$$b^2 = (c_v + k_B/2) k_B T^2, \tag{7}$$

where Δh_v is the bulk enthalpy of vaporization and c_v is the isochoric heat capacity of the vapor [4].

CNT is based on the capillarity approximation: the density of a nucleus is assumed to be the bulk saturated liquid density ρ_ℓ and its surface tension γ_n to be the surface tension of the planar interface γ_∞ [1–4]. Nuclei are assumed to be spherical, thus for one containing n particles the surface area is $A_n = (6\sqrt{\pi} n/\rho_\ell)^{2/3}$.

The surface free energy is related to the surface tension by $\gamma = (\partial\zeta/\partial A)_{p,T}$. The capillarity approximation implies $\zeta_n = \gamma_\infty A_n$. An analysis of experimental results presented by Fenelonov et al. [20] seems to suggest that for some fluids, the surface tension of small nuclei deviates from γ_∞ only by factors between 0.92 and 1.14. Their line of argument is based on the so-called 'first fundamental nucleation theorem' [21]

$$\left(\frac{\partial \ln J}{\partial \ln \mathcal{S}}\right)_T = n^\star + 1, \tag{8}$$

according to which the size of the critical nucleus is obtained from the supersaturation dependence of the nucleation rate at constant temperature. This value of $n^\star$ is then inserted into the Kelvin equation

$$\ln \mathcal{S} = \frac{8\pi\gamma^\star}{3k_BT}\left(\frac{3}{4\pi\rho_\ell}\right)^{2/3}\frac{1}{\sqrt[3]{n^\star}}, \tag{9}$$

a corollary of standard CNT, to obtain the surface tension of the critical nucleus. However, the Kelvin equation does not take any dependence of γ_n on n into account. Hence, it is inconsistent to use this equation for quantifying precisely this size dependence. The nucleation theorem as given in Eq. (8) assumes $d\mu = k_BT d\ln\mathcal{S}$, which is a bad approximation at high temperatures, in particular near the spinodal line. Furthermore, it neglects the dependence of the preexponential coefficient C from Eqs. (3) and (4) on $n^\star$, although C is actually proportional to both p and the surface area of the critical nucleus (cf. Schmelzer [22] for valid forms of the nucleation theorem).

From theoretical considerations [23, 24] and simulations [6, 18] it can be inferred that the surface tension for interfaces with a high curvature is actually much lower. An approximation of the size dependence of the surface tension was given by Tolman [23]

$$\gamma_n = \frac{\gamma_\infty}{1+2\delta/R}, \tag{10}$$

where δ is called the Tolman length and R is the radius of the nucleus. Laaksonen, Ford, and Kulmala (LFK) [25] also proposed a size dependent specific surface energy

$$\zeta_n/A_n = \gamma_\infty(1+\alpha_1 n^{-1/3}+\alpha_2 n^{-2/3}), \tag{11}$$

where α_1 and α_2 are determined from thermal properties. This modification leads to predictions which were found to agree better with simulation data of Tanaka et al. [11] than standard CNT. In the LFK model, the curvature effect is covered by the single parameter α_1, since ΔG_n does not depend on α_2.

INDIRECT APPROACH: CRITICAL NUCLEI FROM MD SIMULATIONS OF EQUILIBRIA

Phase coexistence methods are an established approach for obtaining equilibrium data from molecular simulation [26]. In the present indirect simulation approach, a single nucleus in equilibrium with a supersaturated vapor was studied in the canonical ensemble. For such

simulations it is crucial to choose the relation of the number of particles in the nucleus to the total number of particles in the system appropriately. The liquid fraction must be relatively large so that changes in nucleus size significantly affect the density of the surrounding vapor and the nucleus cannot evaporate completely because the vapor density increases. Eventually, an equilibrium is established, where the nucleus contains n particles while the vapor reaches a supersaturated pressure $p > p_\mathrm{s}$.

Farkas [3] pointed out that for a system with N particles composed of a nucleus containing n and a supersaturated vapor containing $N-n$ particles, an equilibrium between the nucleus and the supersaturated vapor corresponds to the condition $n = n^\star(p,T)$. This is due to the fact that by definition, the Gibbs energy of nucleus formation is maximal for $n^\star(p,T)$ and thus

$$\left(\frac{\partial G_n}{\partial n}\right)_{NpT}\Bigg|_{n=n^\star(p,T)} = 0, \tag{12}$$

holds, which implies that for $n = n^\star(p,T)$, growth and decay are equally probable. Since in a nucleation process ΔG_n has a single maximum [2], this equilibrium condition uniquely identifies the size of the critical nucleus; cf. Mitrović [27] for a discussion of such equilibria in full detail. By minimizing the Helmholtz energy of the system in an NVT simulation, an equilibrium that characterizes the maximum of its Gibbs energy is established. The critical nucleus model of Reguera-Reiss nucleation theory [28] reproduces these considerations in an explicit form.

As suggested by Lovett [29], the fact that a critical nucleus 'can only be in (stable) equilibrium with a supersaturated vapour in a system with a finite (small) volume' makes these small systems where 'the thermodynamic analysis is straightforward and the configurations are easily simulated' an attractive topic for molecular simulation. Such an approach leads to more accurate data on the critical nucleus, e.g. its size $n^\star$ or surface tension $\gamma^\star$, than the usual method of observing growth and decay of nuclei in nonequilibrium simulations [13], because it permits straightforward sampling over a large number of time steps. It is also computationally efficient since only small systems are considered. The molecular simulation of such equilibria is not a novelty in itself [18, 30, 31], but no implications for critical nuclei were drawn from these studies in the past. However, Talanquer [32] used a similar approach based on density functional theory for calculating the free energy of formation and the interfacial density profile of critical nuclei.

Simulations in the canonical ensemble based on these considerations can contribute to the study of nucleation processes indirectly, by reproducing vapor-liquid equilibria instead of the condensation itself. Such indirect simulations were conducted for small systems (total number of particles $N < 2 \times 10^4$) and properties of the critical nucleus at moderate supersaturations were obtained, complementing data from previous work [18]. Nuclei with $10^2 < n < 10^4$ particles were inserted into saturated or moderately supersaturated vapor phases. The nucleus size was tracked by applying a version of the cluster criterion of Rein ten Wolde and Frenkel [33] where a particle is considered as belonging to the nucleus if it has at least four neighbors within a radius of $r \leq 1.5\sigma$.

Surface tension and size of the critical nucleus were determined for six temperature values between 0.65 and 0.95 ε/k_B, cf. Fig. 1 as well as Tabs. I and II. As usual, all numerical results are given in terms of the mass m of a single particle and the two potential parameters σ (size) and ε (energy). The planar interface surface tension γ_∞ of the LJTS fluid, given by [18]

$$\frac{\gamma_\infty \sigma^2}{\varepsilon} = 2.08 \left(1 - \frac{T}{T_\mathrm{c}}\right)^{1.21}, \tag{13}$$

with $T_\mathrm{c} = 1.0779\ \varepsilon/k_B$, is represented by horizontal lines in Fig. 1 because standard CNT assumes the surface tension of the curved interface to be size independent and therefore equal to γ_∞. The surface tension, calculated from the normal component of the Irving-Kirkwood pressure tensor [34], is significantly reduced for small nuclei when compared to γ_∞. Standard CNT neglects this effect, and as shown in Fig. 1, the LFK expression for ζ_n given by Eq. (11) may even lead to values of γ_n for small nuclei which are unphysical, i.e. $\gamma_n > \gamma_\infty$, and increase for smaller nuclei.

Simulation results from our group for $n^\star$ are compared in Fig. 2 to theoretical values. The LFK modification is in better agreement with simulation data over the entire studied temperature range than standard CNT which consistently underestimates $n^\star$ and leads to particularly large deviations at high temperatures.

DIRECT APPROACH: MD SIMULATION OF HOMOGENEOUS NUCLEATION

A series of direct simulations of the nucleation process was conducted in the canonical ensemble using the program ls1 [35]. The system size was relatively large ($10^5 < N < 10^6$) and a hybrid cluster criterion was used to detect the nuclei. This criterion combines

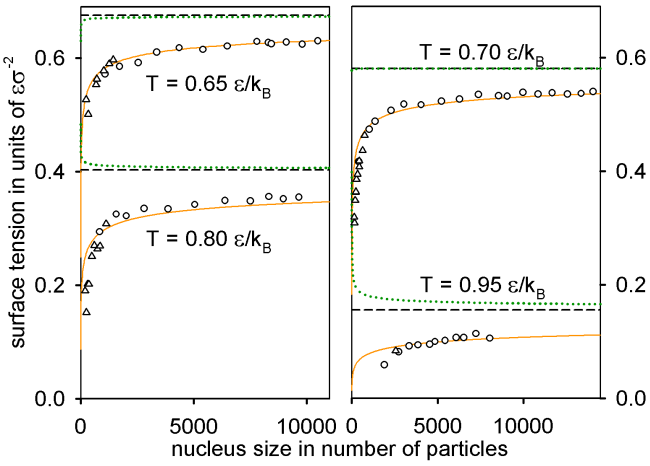

Figure 1: (Color) Surface tension of the LJTS fluid over nucleus size from indirect simulations (△ this work, ∘ from previous work [18]) and following standard CNT (dashed lines), the LFK modification of CNT (dots), and the new SPC modification of CNT (solid lines). The LFK model, which depends on the supersaturated vapor pressure, was evaluated at $\mathcal{S} = 2.86$, 2.28, 1.62, and 1.17 for $T = 0.65$, 0.70, 0.80, and 0.95 ε/k_B, respectively.

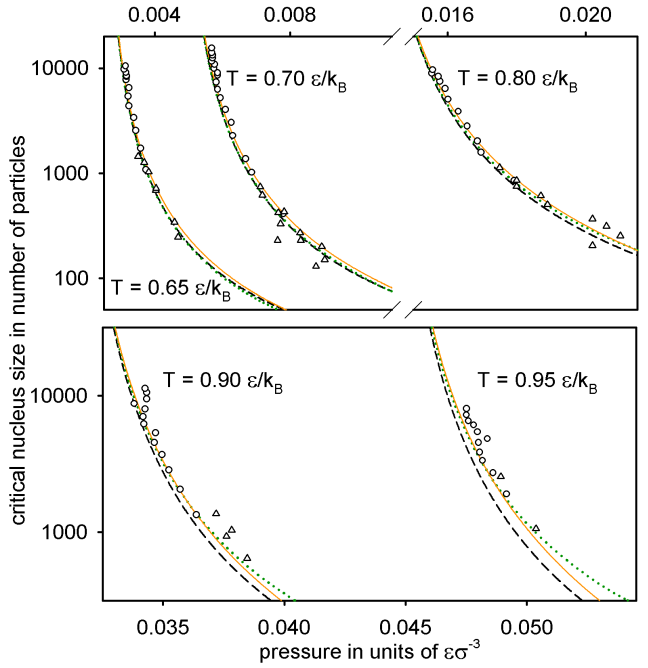

Figure 2: (Color) Critical nucleus size of the LJTS fluid over supersaturated pressure from indirect simulations (△ this work, ∘ from previous work [18]) and following standard CNT (dashed lines), the LFK modification of CNT (dots), and the new SPC modification of CNT (solid lines).

Table I: Size of the critical nucleus (in number of particles) and its surface tension (in units of ε/σ^2) at low temperatures (given in units of ε/k_B) from simulation in comparison to theories – bold values are taken from earlier work [18]

T	$\mathcal{S}$	$n^\star$	$\gamma^\star$	$n^\star$(CNT)	$n^\star$(LFK)	$n^\star$(SPC)
0.65	**1.226**	**10500**	**0.630**	7800	7800	8500
0.65	**1.337**	**3400**	**0.610**	2700	2700	3000
0.65	**1.420**	**1700**	**0.585**	1600	1500	1700
0.65	1.461	1300	0.590	1200	1200	1400
0.65	1.512	1000	0.578	950	940	1100
0.65	1.594	690	0.553	670	660	750
0.65	1.599	720	0.563	650	640	730
0.65	1.813	340	0.501	320	320	360
0.65	1.856	250	0.527	290	280	320
0.70	**1.179**	**15600**	**0.535**	8900	8700	9600
0.70	**1.306**	**2300**	**0.507**	2100	2100	2300
0.70	**1.420**	**1000**	**0.474**	930	930	1100
0.70	1.474	740	0.463	690	690	790
0.70	1.586	420	0.418	410	420	470
0.70	1.621	430	0.408	360	370	410
0.70	1.722	230	0.363	260	260	290
0.70	1.816	130	0.319	200	190	220
0.70	1.869	150	0.309	170	170	190
0.80	**1.125**	**9700**	**0.355**	8000	8300	9100
0.80	**1.179**	**3900**	**0.334**	2900	3100	3400
0.80	**1.227**	**1600**	**0.325**	1500	1600	1800
0.80	1.264	1100	0.308	1000	1100	1200
0.80	1.301	750	0.264	730	790	870
0.80	1.352	610	0.270	490	530	580
0.80	1.366	500	0.251	450	490	520
0.80	1.460	200	0.190	260	280	290
0.80	1.518	250	0.152	190	220	220

Table II: Size of the critical nucleus (in number of particles) and its surface tension (in units of ε/σ^2) at high temperatures (given in units of ε/k_B) from simulation in comparison to theories – bold values are taken from earlier work [18]

T	$\mathcal{S}$	$n^\star$	$\gamma^\star$	$n^\star$(CNT)	$n^\star$(LFK)	$n^\star$(SPC)
0.85	**1.102**	**8800**	**0.268**	7100	7700	8400
0.85	**1.136**	**3000**	**0.250**	3200	3500	3800
0.85	1.152	2200	0.222	2400	2600	2800
0.85	**1.168**	**2200**	**0.240**	1800	2000	2200
0.85	1.227	840	0.202	800	920	970
0.85	1.253	1300	0.224	600	700	730
0.85	1.264	680	0.157	540	630	650
0.85	1.340	450	0.127	290	340	340
0.85	1.424	250	0.072	170	210	190
0.90	**1.086**	**7000**	**0.191**	5600	6400	6800
0.90	**1.111**	**3700**	**0.173**	2700	3200	3400
0.90	**1.134**	**2100**	**0.165**	1600	2000	2000
0.90	1.182	1400	0.132	700	890	880
0.90	1.198	930	0.118	570	730	700
0.90	1.201	1000	0.139	550	700	680
0.90	1.223	650	0.033	410	540	511
0.95	**1.067**	**7200**	**0.114**	4400	5600	5700
0.95	**1.074**	**6100**	**0.107**	3300	4300	4300
0.95	**1.077**	**5400**	**0.102**	3000	3900	3900
0.95	**1.082**	**3400**	**0.092**	2400	3300	3200
0.95	**1.086**	**4800**	**0.100**	2200	2900	2900
0.95	1.099	2600	0.084	1400	2000	1900
0.95	1.104	1900	0.059	1300	1800	1700

geometric and energetic approaches with a connectivity analysis based on graph theory [36]. The nucleation rate was determined by defining a threshold i and counting the number J_i of nuclei containing at least i particles that emerge per volume and time [10]. According to this method, seven nucleation rate isotherms were obtained for temperatures between 0.65 and 1 ε/k_B.

Nucleation rates J_i for different threshold values i are compared to theoretical predictions in Fig. 3 as well as Tabs. III and IV. The values of J_i are only valid approximations of the actual nucleation rate if they remain roughly constant for increasing i [10]. This is the case for all temperatures except 0.95 and 1 ε/k_B where $n^\star$ is probably larger than all of the chosen threshold values. With $n^\star \gg i$, the rate of formation for nuclei with i or more particles does not correspond to the nucleation rate, but rather to the velocity at which the metastable equilibrium which precedes nucleation is established. For instance, at 0.95 ε/k_B and a supersaturation of 1.226, standard CNT predicts a critical nucleus with 173 particles (LFK: $n^\star = 293$); thus, the value of $J_{100} = 3 \times 10^{-7}\sqrt{\varepsilon m^{-1}}/\sigma^4$ obtained under these conditions, cf. Tab. IV, does not describe nucleation but equilibration. Some other results describe the transition between both regimes, such as $J_{400} = 1 \times 10^{-7}\sqrt{\varepsilon m^{-1}}/\sigma^4$ at $T = 1\ \varepsilon/k_B$ and $\mathcal{S} = 1.106$, where the critical size according to CNT is 328 (LFK: $n^\star = 755$).

In those cases where J_i clearly represents the actual nucleation process, consistent deviations were found for standard CNT which underestimates J by two orders of magnitude in all cases. Such an accuracy should be interpreted as a confirmation of standard CNT for the LJTS fluid. The LFK modification is in better agreement with simulation data at low temperatures but leads to larger deviations of J at high temperatures.

SURFACE PROPERTY CORRECTED MODIFICATION OF CNT

As the preceding sections show, standard CNT only predicts the nucleation rate of the LJTS fluid with an acceptable accuracy, leading to deviations for $n^\star$; the LFK modification provides excellent predictions for the critical nucleus size but not for the temperature dependence of J. Both theories assume an inappropriate curvature dependence of the surface tension, although for this essential property of inhomogeneous systems a qualitatively correct expression is known since the 1940s [23]. With the collected simulation data on $\gamma^\star$, $n^\star$, and J over a broad range of temperatures, enough quantitative information is available to

Table III: Nucleation rate (in units of $\sqrt{\varepsilon m^{-1}}/\sigma^4$) at low temperatures (given in units of ε/k_B) from the present simulations in comparison to theories

T	$\mathcal{S}$	J_i	i	J(CNT)	J(LFK)	J(SPC)
0.65	4.14	5×10^{-9}	100	2×10^{-11}	2×10^{-10}	2×10^{-9}
0.65	4.27	7×10^{-9}	25	4×10^{-11}	4×10^{-10}	4×10^{-9}
0.65	5.09	3×10^{-7}	25	9×10^{-10}	1×10^{-8}	5×10^{-8}
0.70	3.06	3×10^{-9}	50	5×10^{-11}	1×10^{-10}	4×10^{-9}
0.70	3.15	1×10^{-8}	150	1×10^{-10}	4×10^{-10}	8×10^{-9}
0.70	3.19	1×10^{-8}	75	1×10^{-10}	5×10^{-10}	1×10^{-8}
0.70	3.22	2×10^{-8}	50	2×10^{-10}	6×10^{-10}	1×10^{-8}
0.70	3.28	8×10^{-8}	150	3×10^{-10}	1×10^{-9}	2×10^{-8}
0.70	3.35	1×10^{-7}	75	4×10^{-10}	2×10^{-9}	3×10^{-8}
0.70	3.39	2×10^{-7}	75	5×10^{-10}	2×10^{-9}	3×10^{-8}
0.70	3.42	3×10^{-7}	75	6×10^{-10}	3×10^{-9}	4×10^{-8}
0.70	3.49	3×10^{-7}	50	1×10^{-9}	4×10^{-9}	5×10^{-8}
0.70	3.55	4×10^{-7}	50	1×10^{-9}	7×10^{-9}	6×10^{-8}
0.80	1.791	2×10^{-9}	25	5×10^{-12}	2×10^{-13}	5×10^{-10}
0.80	1.792	1×10^{-9}	50	6×10^{-12}	3×10^{-13}	5×10^{-10}
0.80	1.792	8×10^{-10}	75	6×10^{-12}	3×10^{-13}	5×10^{-10}
0.80	1.869	8×10^{-9}	50	5×10^{-11}	4×10^{-12}	3×10^{-9}
0.80	1.869	3×10^{-9}	75	5×10^{-11}	4×10^{-12}	3×10^{-9}
0.80	1.885	4×10^{-8}	25	7×10^{-11}	7×10^{-12}	5×10^{-9}
0.85	1.539	3×10^{-8}	600	2×10^{-11}	9×10^{-14}	1×10^{-9}
0.85	1.550	2×10^{-9}	300	3×10^{-11}	2×10^{-13}	2×10^{-9}
0.85	1.560	4×10^{-9}	600	6×10^{-11}	3×10^{-13}	2×10^{-9}
0.85	1.560	7×10^{-8}	600	6×10^{-11}	3×10^{-13}	2×10^{-9}
0.85	1.566	1×10^{-8}	300	7×10^{-11}	4×10^{-13}	3×10^{-9}
0.85	1.596	1×10^{-8}	100	2×10^{-10}	3×10^{-12}	8×10^{-9}
0.85	1.647	2×10^{-7}	300	9×10^{-10}	3×10^{-11}	3×10^{-8}
0.85	1.656	1×10^{-7}	100	1×10^{-9}	4×10^{-11}	3×10^{-8}

Table IV: Nucleation rate (in units of $\sqrt{\varepsilon m^{-1}}/\sigma^4$) at high temperatures (given in units of ε/k_B) from the present simulations in comparison to theories

T	$\mathcal{S}$	J_i	i	J(CNT)	J(LFK)	J(SPC)
0.90	1.31	6×10^{-9}	75	3×10^{-12}	9×10^{-17}	4×10^{-11}
0.90	1.34	1×10^{-8}	100	3×10^{-11}	3×10^{-15}	6×10^{-10}
0.90	1.35	4×10^{-8}	50	7×10^{-11}	8×10^{-15}	1×10^{-9}
0.90	1.36	8×10^{-9}	200	1×10^{-10}	2×10^{-14}	2×10^{-9}
0.90	1.37	5×10^{-8}	50	2×10^{-10}	6×10^{-14}	4×10^{-9}
0.90	1.38	2×10^{-8}	200	4×10^{-10}	2×10^{-13}	7×10^{-9}
0.90	1.39	2×10^{-7}	50	6×10^{-10}	3×10^{-13}	1×10^{-8}
0.90	1.39	1×10^{-7}	75	6×10^{-10}	3×10^{-13}	1×10^{-8}
0.90	1.39	6×10^{-8}	100	6×10^{-10}	3×10^{-13}	1×10^{-8}
0.95	1.159	2×10^{-8}	100	1×10^{-13}	3×10^{-22}	2×10^{-13}
0.95	1.172	4×10^{-7}	50	2×10^{-12}	3×10^{-20}	5×10^{-12}
0.95	1.198	1×10^{-7}	100	7×10^{-11}	3×10^{-17}	4×10^{-10}
0.95	1.211	8×10^{-9}	700	3×10^{-10}	3×10^{-16}	2×10^{-9}
0.95	1.218	2×10^{-8}	300	5×10^{-10}	1×10^{-15}	4×10^{-9}
0.95	1.221	2×10^{-7}	100	7×10^{-10}	2×10^{-15}	5×10^{-9}
0.95	1.226	3×10^{-7}	100	1×10^{-9}	4×10^{-15}	8×10^{-9}
0.95	1.237	2×10^{-6}	50	2×10^{-9}	2×10^{-14}	2×10^{-8}
1.00	1.039	5×10^{-8}	150	2×10^{-31}	3×10^{-59}	1×10^{-39}
1.00	1.044	5×10^{-7}	50	4×10^{-26}	1×10^{-50}	5×10^{-32}
1.00	1.044	4×10^{-8}	150	4×10^{-26}	1×10^{-50}	5×10^{-32}
1.00	1.057	1×10^{-7}	150	4×10^{-18}	9×10^{-37}	9×10^{-21}
1.00	1.061	8×10^{-8}	150	1×10^{-16}	5×10^{-34}	1×10^{-18}
1.00	1.065	4×10^{-7}	75	2×10^{-15}	1×10^{-31}	7×10^{-17}
1.00	1.072	5×10^{-7}	75	1×10^{-13}	3×10^{-28}	2×10^{-14}
1.00	1.106	1×10^{-7}	400	1×10^{-9}	5×10^{-19}	4×10^{-9}
1.00	1.108	5×10^{-8}	800	2×10^{-9}	1×10^{-18}	6×10^{-9}

formulate a more adequate modification of CNT.

To correlate the simulation results for $\gamma^\star$, Eq. (10) as proposed by Tolman [23] was chosen. The quotient δ/R was assumed to scale with $n^{-1/3}$, and a fit to the data shown in Fig. 1 as well as Tabs. I and II yields

$$\delta/R = \left(\frac{0.7}{1 - T/T_\mathrm{c}} - 0.9 \right) / n^{1/3}. \tag{14}$$

It can be seen in Fig. 1 that the two-parameter fit given by Eqs. (10) and (14) is sufficient to reproduce both temperature and size dependence of the surface tension.

The new SPC modification of CNT is based on a size dependent term for the surface tension, given by Eqs. (10) and (14) for the LJTS fluid. From theoretical considerations [4] and from simulation [37] it is further known that the number of particles n in the nucleus is insufficient as a reaction coordinate for nucleation. In particular, the external shape and – in case of liquid-solid nucleation – the internal structure of the nuclei must be taken into account [37, 38]. An MD based analysis of the emerging crystals in a supercooled LJ liquid by Trudu et al. [14] showed that for liquid-solid nucleation, the nuclei are significantly anisotropic: the longest axis of the ellipsoids used to approximate the crystal surface was found to be about 1.5 times longer than the shortest axis.

The nonsphericity of the nuclei in a supersaturated vapor, due to fluctuations of the phase boundary, is represented by a size dependent steric coefficient s_n with

$$A_n = s_n \left(6\sqrt{\pi} n / \rho_\ell \right)^{2/3}, \tag{15}$$

in the present SPC modification of CNT. The temperature and size dependence of s_n was accounted for by a two-parameter fit

$$s_n = \frac{0.85 \left(1 - T/T_\mathrm{c}\right)^{-1} + (n/75)^{1/3}}{1 + (n/75)^{1/3}}, \tag{16}$$

adjusted to all simulation results for $n^\star$ and J. This corresponds to an effective increase of the radius according to capillarity theory $R_\mathrm{cap} = \sqrt[3]{3/(4\pi\rho_\ell)}$ by a factor of $\sqrt{s_n}$. As Fig. 4 shows, this increase is similar in magnitude to phyiscal properties that express the size of the phase boundary, such as the Tolman length δ and the interface thickness on the vapor side D^ϱ_v determined from the average density profile of the nucleus. Both properties were studied for the LJTS fluid in previous work [18].

For all temperatures above 0.162 ε/k_B, which is far below the triple point temperature (about 0.61 ε/k_B), Eq. (16) leads to $s_n > 1$. For $T \to T_\mathrm{c}$, both the steric coefficient and the

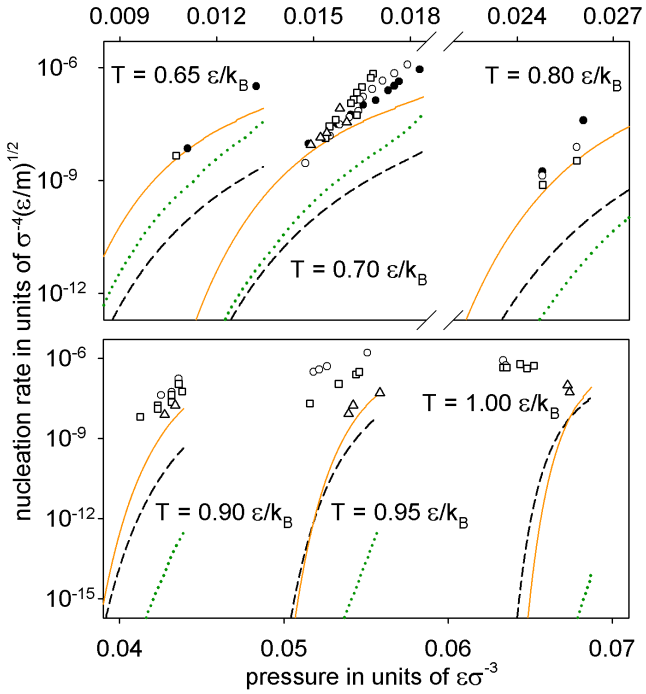

Figure 3: (Color) Nucleation rate of the LJTS fluid over supersaturated pressure from the present direct simulations for different threshold values ($\bullet$ $i = 25$, $\circ$ $i = 50$, $\square$ $i \in \{75, 100\}$, $\triangle$ $i \geq 150$) and following standard CNT (dashed lines), the LFK modification of CNT (dots), and the new SPC modification of CNT (solid lines).

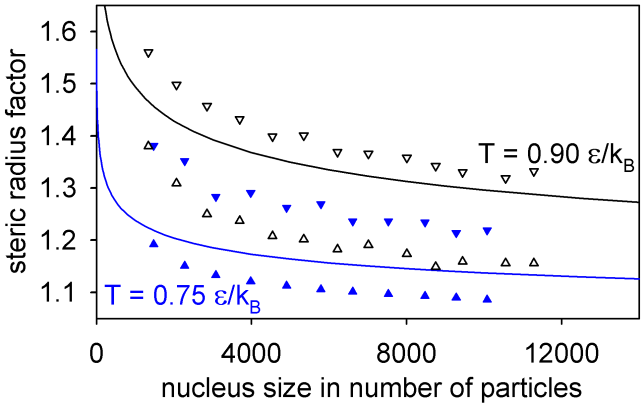

Figure 4: (Color) Steric radius factor $\sqrt{s_n}$ in dependence of the nucleus size n at temperatures of 0.75 and 0.90 ε/k_B (solid lines); values from previous work [18] are shown for $1 + \delta/R_{\text{cap}}$ (triangle up) and $1 + D_{\text{v}}^{\rho}/R_{\text{cap}}$ (triangle down) at 0.75 (filled symbols) and 0.90 (empty symbols) ε/k_B

thickness of the vapor-liquid interface diverge. It should be noted that in the case of fluids that cannot be accurately modeled by the truncated and shifted LJ potential, the surface tension of small nuclei and the thickness of the phase boundary may require a different set of parameters for Eqs. (14) and (16).

As can be seen from Figs. 1 – 3, the SPC modification consistently covers the LJTS simulation results for $\gamma^\star$, $n^\star$, and J. At the transition between nucleation and spinodal decomposition, the nucleation rates from simulation exceed the prediction by about an order of magnitude, which may be due to the particular energy landscape of such processes [39]. The apparent difference between the values of J_i and all theories at temperatures of 0.95 and 1 ε/k_B is due to the fact that as discussed above, almost all of these values describe the velocity of equilibration instead of nucleation.

APPLICATION TO ARGON

Fluid argon can be represented accurately by an LJTS molecular model, the corresponding potential parameters were determined as $\sigma = 3.3916$ Å and $\varepsilon/k_B = 137.90$ K in previous work [18]. Conveniently, experimental nucleation data are available, however, usually at very low temperatures below the triple point. The onset pressure p_{on}, defined as the pressure where the nucleation rate exceeds a certain minimal value J_{on}, was determined for the homogeneous nucleation of argon by Pierce et al. [40], Zahoranski et al. [41, 42], and Iland et al. [43]. The onset nucleation rate J_{on} depends on the experimental setup and was provided (or estimated) by the authors of the respective studies, except for Pierce et al. [40], where we assumed $J_{\mathrm{on}} = 10^{22}$ m^{-3}s^{-1} as given by Iland [8] for the nucleation rate detected by supersonic nozzles.

The comparison between theory and experiment is inconclusive and appears contradictory, cf. Tab. V. Results obtained by Pierce et al. [40] tend to confirm CNT. Zahoranski et al. [41] observed a nucleation onset at much lower pressures than all theories. A second study by Zahoranski et al. [42] agrees best with the SPC modification, whereas the correlation proposed by Iland et al. [43] confirms LFK. However, it should be pointed out that at such very low temperatures (60 to 70% of the triple point temperature) desublimation processes take place. Therefore, such severe extrapolations to other parts of the phase diagram are questionable.

CONCLUSION

The present simulation results show for the LJTS fluid that standard CNT underpredicts the nucleation rate J at high supersaturations by about two orders of magnitude. The critical nucleus size $n^\star$ is also lower by up to a factor of two at moderate supersaturations. The LFK modification is an improvement with respect to $n^\star$, but leads to large deviations for J at high temperatures. A surface property corrected modification of CNT was presented that takes into account the lower surface tension of small nuclei and their nonsphericity, effects ignored by standard CNT. This modification consistently reproduces simulation data for $\gamma^\star$, $n^\star$, and J over a wide range of states.

We thank Martin Bernreuther, Karlheinz Schaber, Nicolas Schmidt, Jonathan Walter, and Andrea Wix for fruitful discussions and Deutsche Forschungsgemeinschaft for funding Sonderforschungsbereich 716. The simulations were performed on the HP XC6000 super computer at the Steinbuch Centre for Computing, Karlsruhe under the grant MMSTP.

---

* Author to whom correspondence should be addressed: J. Vrabec; Electronic address: `vrabec@itt.uni-stuttgart.de`

[1] J. W. Gibbs, *Collected Works. Vol 1. Thermodynamics* (Longmans, Green & Co., London, 1878).

[2] M. Volmer and A. Weber, Z. phys. Chem. (Leipzig) **119**, 277 (1926).

[3] L. Farkas, Z. phys. Chem. (Leipzig) **125**, 236 (1927).

[4] J. Feder, K. C. Russell, J. Lothe, and G. M. Pound, Adv. Phys. **15**, 111 (1966).

[5] I. J. Ford, Proc. Inst. Mech. Eng. C: J. Mech. Eng. Sci. **218**, 883 (2004).

[6] J. Merikanto, E. Zapadinsky, H. Vehkamäki, and A. Lauri, Phys. Rev. Lett. **98**, 145702 (2007).

[7] M. Kulmala, Science **302**, 1000 (2003).

[8] K. Iland, Ph.D. thesis, University of Cologne (2004).

[9] P. G. Debenedetti, Nature **441**, 168 (2006).

[10] K. Yasuoka and M. Matsumoto, J. Chem. Phys. **109**, 8451 (1998).

[11] K. K. Tanaka, K. Kawamura, H. Tanaka, and K. Nakazawa, J. Chem. Phys. **122**, 184514 (2005).

[12] T. S. van Erp, D. Moroni, and P. G. Bolhuis, J. Chem. Phys. **118**, 7762 (2003).

[13] D. I. Zhukovitskii, J. Chem. Phys. **103**, 9401 (1995).

[14] F. Trudu, D. Donadio, and M. Parrinello, Phys. Rev. Lett. **97**, 105701 (2006).

[15] H. Wang, H. Gould, and W. Klein, Phys. Rev. E **76**, 031604 (2007).

[16] M. P. Allen and D. J. Tildesley, *Computer Simulation of Liquids* (Clarendon, Oxford, 1987).

[17] C. Ibergay, A. Ghoufi, F. Goujon, P. Ungerer, A. Boutin, B. Rousseau, and P. Malfreyt, Phys. Rev. E **75**, 051602 (2007).

[18] J. Vrabec, G. K. Kedia, G. Fuchs, and H. Hasse, Mol. Phys. **104**, 1509 (2006).

[19] M. Blander and J. L. Katz, J. Stat. Phys. **4**, 55 (1972).

[20] V. B. Fenelonov, G. G. Kodenyov, and V. G. Kostrovsky, J. Phys. Chem. B **105**, 1050 (2001).

[21] I. J. Ford, Phys. Rev. E **56**, 5615 (1997).

[22] J. W. P. Schmelzer, J. Coll. Interf. Sci. **242**, 354 (2001).

[23] R. C. Tolman, J. Chem. Phys. **17**, 333 (1949).

[24] V. G. Baidakov and G. S. Boltachev, Phys. Rev. E **59**, 469 (1999).

[25] A. Laaksonen, I. J. Ford, and M. Kulmala, Phys. Rev. E **49**, 5517 (1994).

[26] J. R. Morris, C. Z. Wang, K. M. Ho, and C. T. Chan, Phys. Rev. B **49**, 3109 (1994).

[27] J. Mitrovic, Chem. Eng. Sci. **61**, 5925 (2006).

[28] D. Reguera and H. Reiss, Phys. Rev. Lett. **93**, 165701 (2004).

[29] R. Lovett, Rep. Prog. Phys. **70**, 195 (2007).

[30] P. Schaaf, B. Senger, J.-C. Voegel, R. K. Bowles, and H. Reiss, J. Chem. Phys. **114**, 8091 (2001).

[31] M. Salonen, I. Napari, and H. Vehkamäki, Mol. Sim. **33**, 245 (2007).

[32] V. Talanquer, J. Phys. Chem. B **111**, 3438 (2007).

[33] P. Rein ten Wolde and D. Frenkel, J. Chem. Phys. **109**, 9901 (1998).

[34] J. H. Irving and J. G. Kirkwood, J. Chem. Phys. **18**, 817 (1950).

[35] M. Bernreuther and J. Vrabec, in *High Performance Computing on Vector Systems*, edited by M. Resch et al. (Springer, 2006), pp. 187–195.

[36] S. Grottel, G. Reina, J. Vrabec, and T. Ertl, IEEE Trans. Vis. Comp. Graph. **13**, 1624 (2007).

[37] D. Moroni, P. Rein ten Wolde, and P. G. Bolhuis, Phys. Rev. Lett. **94**, 235703 (2005).

[38] E. Sanz, C. Valeriani, D. Frenkel, and M. Dijkstra, Phys. Rev. Lett. **99**, 055501 (2007).

[39] P. Bhimalapuram, S. Chakrabarty, and B. Bagchi, Phys. Rev. Lett. **98**, 206104 (2007).

[40] T. Pierce, P. M. Sherman, and D. D. McBride, Astronautica Acta **16**, 1 (1971).

[41] R. A. Zahoranski, J. Höschele, and J. Steinwandel, J. Chem. Phys. **103**, 9038 (1995).

[42] R. A. Zahoranski, J. Höschele, and J. Steinwandel, J. Chem. Phys. **110**, 8842 (1999).

[43] K. Iland, J. Wölk, R. Strey, and D. Kashchiev, J. Chem. Phys. **127**, 154506 (2007).

Table V: Nucleation onset pressure p_{on} (in units of kPa) for argon at low temperatures (in units of K) from experimental data in comparison to the pressure where the assumed onset nucleation rate J_{on} (in units of $\mathrm{m}^{-3}\mathrm{s}^{-1}$) is reached according to theories; the data of Pierce et al. [40] were published in graphical form only

ref.	T	p_{on}(exp)	p_{on}(CNT)	p_{on}(LFK)	p_{on}(SPC)	J_{on}
[41]	48.2	0.31	1.2	0.83	1.3	10^{6}
[43]	48.2	1.3	2.1	1.4	2.1	10^{13}
[40]	55	19	16	14	14	10^{22}
[41]	55.8	0.99	4.8	6.0	4.8	10^{6}
[42]	55.9	5.28	6.7	7.2	6.5	10^{12}
[43]	55.9	6.2	7.1	7.5	6.9	10^{13}
[42]	60.2	11.1	12	13	12	10^{12}
[41]	60.3	2.27	9.5	11	9.3	10^{6}
[42]	62.7	12.7	17	17	17	10^{12}
[40]	63	52	34	29	30	10^{22}
[42]	69.9	23.9	42	40	40	10^{12}
[41]	85.1	114	180	180	180	10^{6}
[40]	98	690	570	570	540	10^{22}